

## Mechanical properties of aluminum-based nanocomposite reinforced with fullerenes

Kwangmin CHOI<sup>1</sup>, Jiyeon SEO<sup>2</sup>, Donghyun BAE<sup>2</sup>, Hyunjoo CHOI<sup>1</sup>

1. School of Advanced Materials Engineering, Kookmin University, Seoul 136-702, Korea;

2. School of Advanced Materials Engineering, Yonsei University, Seoul 120-749, Korea

Received 18 June 2013; accepted 14 October 2013

**Abstract:** The strengthening effect of fullerenes in aluminum matrix composites was investigated. The composites are produced using a two-step ball-milling technique combined with a hot rolling process. First, fullerene aggregates, where fullerene molecules initially come together to form giant particles (~200  $\mu\text{m}$  in diameter) via van der Waals bonding, are shattered into smaller particles (~1  $\mu\text{m}$  in diameter) by planetary milling. Second, primarily ball-milled fullerenes are dispersed in aluminum powder via attrition milling. Finally, aluminum/fullerene composite powder is consolidated by hot-rolling at 480 °C. For the composite sheet, grain refinement strengthening and dispersion hardening by fullerenes are accomplished at the same time, thereby exhibiting HV ~222 of Vickers hardness (e.g., ~740 MPa of yield strength) with only 2% (volume fraction) of fullerenes.

**Key words:** aluminum; fullerenes; ball-milling; powder metallurgy; composites

### 1 Introduction

One strategy to increase energy efficiencies is the development of new structural materials with high specific mechanical performance. Aluminum, which is earth abundant and is easy to process, has been spot-lighted as light-weight structural parts in automotive [1], aerospace [2], electronic industries [3], due to its low density and consequently weight-saving potential. Aluminum matrix composites with these advantages, making up for its low strength/stiffness limitations, have been of great interest [4–19].

Carbon nano-materials, such as fullerenes [4,5], carbon nanotubes [6–17], and graphenes [18,19], have so far been well attended as reinforcements for the aluminum matrix composites, due to their lightweight nature and superior strength/stiffness stemming from strong  $\text{sp}^2$  C—C bonds [20]. Hence, numerous fabrication methods have been proposed to develop metal matrix composites containing carbon nano-materials by means of liquid-state techniques [5–11] as well as solid-state techniques [13–17]. Spraying processes [6–8], squeeze casting [9], and disintegrated melt deposition [10,11] processes have been introduced to fabricate the

composite at temperatures above the melting temperature of the matrix. Carbon nano-materials are initially entangled or agglomerated via van der Waals bonds, and hence they are not easily dispersed each by each in the melt of the matrix. Therefore, solid-state techniques have been considered as more promising routes, enabling mechanical dispersion of these nano-scale materials into metals via severe plastic deformation of the metal matrix [12–17]. However, it has been reported that the significant damage of carbon nano-materials during processes with severe mechanical energy results in unfavorable chemical interfacial reactions between the damaged carbon nano-materials and the metal matrix during high-temperature consolidation processes [16,17]. Without solving this critical problem in dispersion, therefore, the giga-Pascal-level strength of the carbon nano-materials would not be beneficial for any structural composite application [12–17].

With this scope, fullerenes with a spherical structure may be considered as a more fascinating reinforcements compared with carbon nanotubes or graphenes, due to their zero-dimensional geometric characteristics. They would be readily dispersed and rarely destroyed during severe mechanical dispersion processes in the metal matrix. Previously, TOKUNAGA et al [4] have reported

the improvement of yield strength of aluminum from 150 to 250 MPa by reinforcing fullerenes via severe plastic deformation. KHALID et al [5] has developed aluminum-based composites via liquid metal infiltration, where the composite shows good interfacial bonding between aluminum and fullerenes. However, the mechanical properties of the composites are still below the theoretical expectation compared with the superior stiffness/strength of fullerenes.

In this work, we employ two-step ball-milling techniques to disperse fullerenes into the aluminum matrix. In the first stage, fullerene aggregates are shattered into small particles using two different control agents. In the second stage, the shattered fullerenes are dispersed into aluminum powder using a high-energy ball milling technique, at which the grain size of aluminum is reduced down to tens of nanometers at the same time. Eventually, the composite powder is consolidated to a sheet-type composite using a hot-rolling process and strengthening efficiency of fullerenes in the aluminum matrix composite is investigated.

## 2 Experimental

Aluminum-based composites containing fullerenes were fabricated by hot-rolling of ball-milled powder. Aluminum powder (150  $\mu\text{m}$ , 99.5% in purity, Changsung Co. Ltd.) and fullerene soot (Sigma Aldrich Korea Co. Ltd.) were used as starting materials. Although the diameter of an individual fullerene molecule is about 1 nm, the molecules come together to form giant particles (~200  $\mu\text{m}$  in diameter) with the long-range periodicity of the face-centered cubic (FCC) crystalline structure during manufacturing (Fig. 1(a)).

Ball milling was conducted via two steps of planetary milling followed by attrition milling. A planetary mill (Fritsch Co. Ltd., Pulverisette 5, Germany) was employed to shatter fullerene aggregates where fullerenes are initially agglomerated via van der Waals bonding [21]. In this grinding operation, the solid–solid contact among fullerene aggregates provides the friction, breaking the weak van der Waals bonds among fullerenes without severe destruction of their initial molecular structure. The effect of two different control agents on this shattering operation was compared: 10% (mass fraction) stearic acid as a solid control agent was employed to prevent agglomeration among fullerenes, and 95.0% ethyl alcohol as a liquid control agent was used to weaken the bonds among fullerenes as well as to prevent agglomeration. A stainless steel chamber (500 mL) was charged with 1 g of fullerenes and 800 g of 5 mm-diameter-stainless balls together with a control agent. Then, a cycle of 200 r/min milling for 15 min and pausing for 75 min was repeated 8 times.

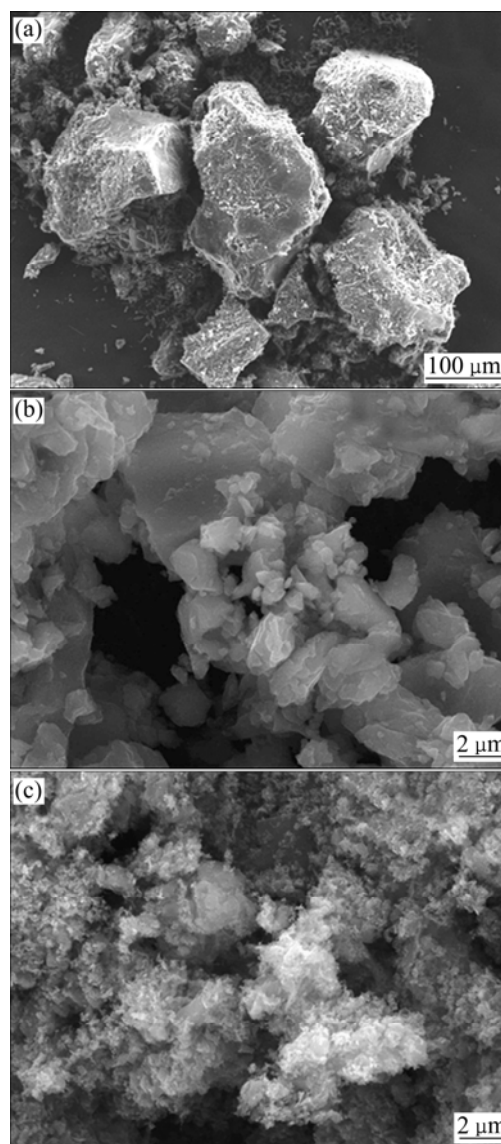


**Fig. 1** SEM images: (a) Pristine fullerenes; (b) Fullerenes after planetary milling with stearic acid; (c) Fullerenes after planetary milling with ethyl alcohol

An attrition mill (KMC Co. Ltd., KMC-1BV, Korea) was used for dispersing shattered fullerenes into aluminum powder. First, a stainless chamber was charged with fullerenes, aluminum powder, and 5 mm-diameter-stainless balls, where the ball-to-powder mass ratio was 15:1. Second, attritor was operated at 500 r/min for 24 h in argon atmosphere. During milling, significant impact energy is induced on powder and hence the powder undergoes severe plastic deformation, dispersing fullerenes into aluminum powder. At the same time, powder sticks to balls, chamber wall and itself. To avoid this excessive cold welding, 1% (mass fraction) stearic acid was used as a process control agent.

Three different powders were finally prepared. Sample A is monolithic aluminum powder ball-milled for

24 h; Sample B is a composite, where fullerenes were first shattered using planetary milling with 10% (mass fraction) stearic acid and then were dispersed in aluminum powder via 2 h planetary milling followed by 24 h attrition milling; Sample C is a composite, where fullerenes were solely planetary-milled as in Sample B, but with ethyl alcohol, and then were dispersed in aluminum powder via the same process as in sample B. For Sample C, ethyl alcohol was vaporized before attrition milling.

Flowingly, sheet-type samples were fabricated by hot rolling of ball-milled powder. Prior to hot rolling, the ball-milled powder was heat-treated at 500 °C in vacuum for 20 min to remove stearic acid. A copper tube was used as a container of powder for rolling. Powder was charged in one-side-sealed copper tube, cold-pressed, and then the other side was sealed. Hot rolling was performed at 480 °C with every 12% of reduction until the thickness of the sample reaches 1.8 mm. The copper container was mechanically peeled off.

The morphology of fullerenes and aluminum powder was observed by scanning electron microscope (SEM, JEOL, JSM 2001F, Japan). Raman spectroscopy (LabRam Aramis, Horiba Jobin Yvon Co. Ltd., France) was used to investigate the Raman spectra of fullerenes in composites. The spectra were collected under ambient conditions using the 514.532 nm line of an argon-ion laser at 0.5 mW power. The grain size of aluminum and composites was calculated using Scherrer equation, based on X-ray diffraction (XRD, Rigaku Ultima III

X-ray diffractometer) analysis with a Cu  $K_{\alpha}$  radiation source. XRD patterns were collected in the range from 20° to 100° with a slit speed of 2 (°)/min. Hardness of aluminum and composites was measured by micro Vickers hardness tester (Mitutoyo, HM-211, Japan) with 3 N load.

### 3 Results and discussion

Figures 1(a)–(c) show SEM images of pristine fullerenes (Fig. 1(a)) and fullerenes after planetary milling with stearic acid (for Sample B, Fig. 1(b)) or ethyl alcohol (for Sample C, Fig. 1(c)). Most fullerene aggregates in Sample B still remain their FCC crystalline periodicity, exhibiting wide size distribution from ~0.1 to 8  $\mu\text{m}$ , as shown in Fig. 1(b). On the other hand, most aggregates in Sample C are segmented into tiny particles with sizes less than 500 nm, as shown in Fig. 1(c). Ethyl alcohol has been reported to be effective to weaken the van der Waals force among fullerenes [22], thereby stimulating de-bonding of fullerenes.

Figure 2 shows SEM images of composite powder, obtained after planetary milling, for Sample B (Fig. 2(a)) and its magnified image (Fig. 2(b)) together with that for Sample C (Fig. 2(c)) and its magnified image (Fig. 2(d)), respectively. Both composite powders in Figs. 2(a) and (c) exhibit similar sizes (from ~60 to 120  $\mu\text{m}$ ) and spherical morphologies. Regarding the size (~150  $\mu\text{m}$ ) and shape of starting aluminum powder, the powder seems to be rarely refined or deformed during planetary

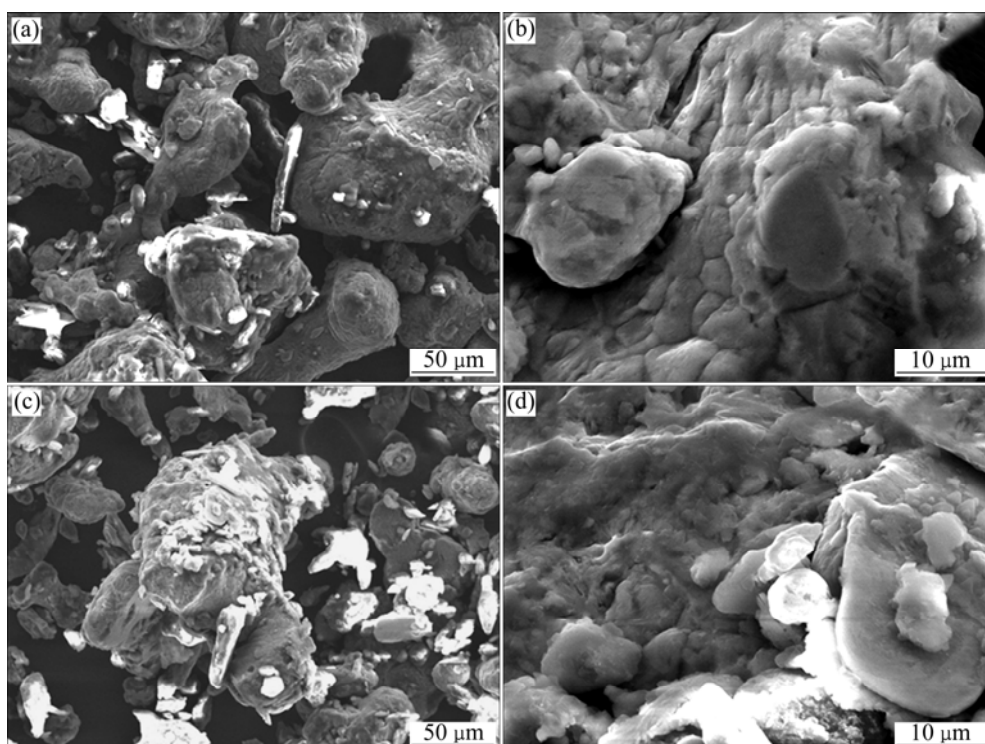


**Fig. 2** SEM images of composite powder obtained after planetary milling: (a) Sample B; (b) Magnified image of (a); (c) Sample C; (d) Magnified image of (c)

milling. Impact energy on powder is considered to be insufficient to induce fracturing or flattening of powder. In the magnified images of Figs. 2(b) and (d), fullerene aggregates are rarely detectable on the surface of composite powders. Hence, it is hypothesized that they tend to be embedded inside aluminum powder rather than to physically adhere on the surface of powder.

Raman spectroscopy was performed to assure the presence of fullerenes in the composite and to check the damage level of fullerenes. Figure 3 shows the Raman spectra for a simple mixture of 2% (volume fraction) fullerene soot aluminum powder, Sample B and Sample C, respectively. The simple mixture shows a typical Raman spectrum for fullerene soot where two major peaks are seen based on the different characteristics; the D peak at  $\sim 1330\text{ cm}^{-1}$  represents the disordered non-graphitizable carbon and the G peak at  $\sim 1590\text{ cm}^{-1}$  indicates the graphitic layered structures [23]. Another peak at  $\sim 1468\text{ cm}^{-1}$  may suggest the presence of spherical structure in  $C_{60}$ -fullerenes [24]. As the composite powder is severely milled, peaks shift toward the higher wave number, possibly originating from the compressive force in fullerene soot by a high-velocity impact of balls on the powder [25]. Furthermore, a number of defects might be generated due to the severe ball–powder–ball collision, providing a higher intensity of D peak over G peak for the ball-milled specimens. Despite of the defect generation, Raman characterization confirms the retention of the initial structure of fullerene soot as well as the presence of fullerene soot.

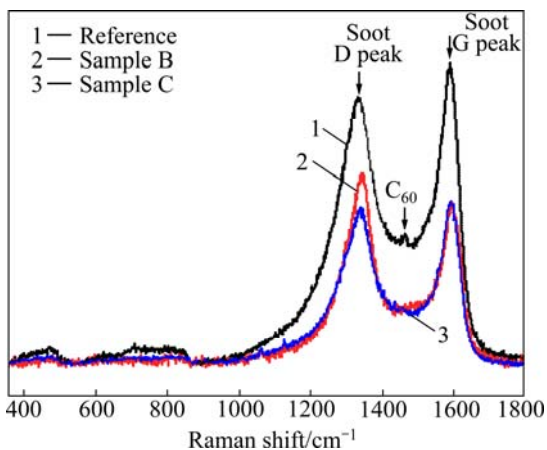


**Fig. 3** Raman spectra of a simple mixture of 2% (volume fraction) fullerene soot, Sample B and Sample C

We consider that strengthening of composites in this work is mainly accomplished with a cooperation of grain refinement of the matrix and load bearing of fullerene soot. To exclude the contribution of grain refinement to the strength, the grain size of composites was measured by XRD. Figure 4 shows the XRD patterns for samples A, B and C. They all exhibit similar peak intensity and

broadening. Based on the patterns, the grain size of samples A, B and C is calculated to be 67, 30, and 29.4 nm, respectively. Although each sample experiences different milling processes, the total time for attrition milling is fixed to be 24 h and hence the effect of milling parameters on the grain refinement is thought to be insignificant. However, fullerenes may play a significant role in stimulating grain refinement during milling as well as in preventing grain growth during hot working processes, resulting in smaller grain sizes of the composite compared with monolithic aluminum.

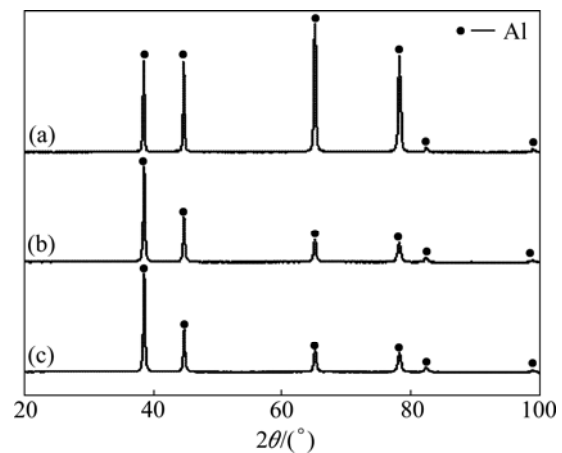


**Fig. 4** XRD patterns: (a) Sample A; (b) Sample B; (c) Sample C

As shown in Fig. 5, the Vickers hardness of samples A, B and C is measured to be HV 130, HV 222.3 and HV 205.5, respectively. It can be converted to the yield strength, based on empirical equation of  $\sigma_y = \sim HV3.3$  for materials with negligible work hardening [26] where  $\sigma_y$  is the yield strength; it is calculated to be  $\sim 470$ ,  $\sim 740$  and  $\sim 685$  MPa for samples A, B and C, respectively. The yield strengths of nanocrystalline aluminum with grain sizes of  $\sim 65$  and  $\sim 30$  nm have been reported to be  $\sim 360$  and  $\sim 480$  MPa, respectively [27]. Note that the yield strength of aluminum follows inverse Hall–Petch relation as the grain size of aluminum is smaller than  $\sim 40$  nm, providing less difference between the yield strength of aluminum with  $\sim 65$  and  $\sim 30$  nm compared with theoretical expectation based on Hall–Petch relation [27]. The difference between the yield strength of monolithic aluminum in the present work and that in the previous report may be due to different residual stress and porosity of samples stemming from different processing routes. Even regarding the differences in grain refinement strengthening for monolithic aluminum and composites, it is considered that fullerenes also play a significant role in strengthening. The composite with only 2% (volume fraction) fullerenes shows HV  $\sim 222$  of Vickers hardness and possibly  $\sim 740$  MPa of yield strength, which are

notable with a consideration of the yield strength of starting aluminum (e.g., ~40 MPa [28]). Although the shattering of fullerenes seems to be better when we use ethyl alcohol as a milling agent, Sample B, produced with stearic acid as a milling agent, shows higher hardness than Sample A. With the help of mechanical energy, ethyl alcohol may change the structural characteristics of fullerenes. This gap may also originate from differences in other parameters such as porosity of samples. Further study is required.

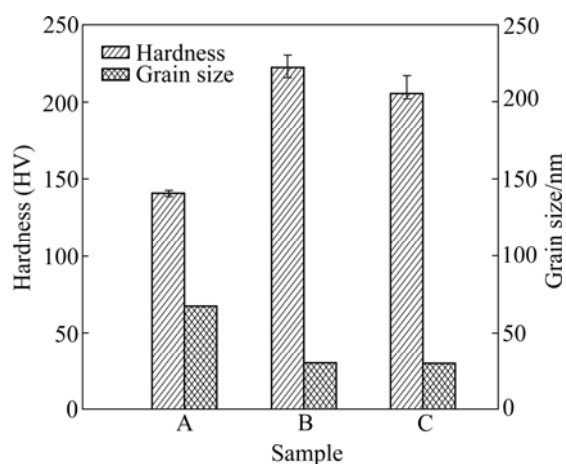


Fig. 5 Vickers hardness and grain size of samples

## 4 Conclusions

Aluminum matrix composite powder was fabricated by two-step ball-milling processes followed by a hot-rolling process. Fullerenes are shattered into smaller particles with the help of control agent in the first stage of milling and then the shattered fullerenes are embedded and dispersed inside aluminum powder in the second stage of milling. For the composite sheet, grain refinement strengthening and dispersion hardening by fullerenes are accomplished at the same time, thereby exhibiting HV ~222 of Vickers hardness (e.g., ~740 MPa of yield strength) with only 2% (volume fraction) of fullerenes.

## Acknowledgement

This work was supported in part by the New Faculty Research Program 2012 of Kookmin University in Korea. Hyunjoo Choi also acknowledges the support from the Priority Research Centers Program (2012-0006680) and the Korea-Belarus Joint Research Program (2012-057348) through the National Research Foundation of Korea (NRF) funded by the Ministry of Education, Science and Technology.

## References

[1] SCHIMEK M, SPRINGER A, KAIERLE S, KRACHT D,

WESLING V. Laser-welded dissimilar steel-aluminum seams for automotive lightweight construction [J]. *Physics Procedia*, 2012, 39: 43–50.

[2] IMMARIGEON J P, HOLT R T, KOUL A K, ZHAO L, WALLACE W, BEDDOES J C. Lightweight materials for aircraft applications [J]. *Materials Characterization*, 1995, 35(1): 41–67.

[3] JIA Q J, LIU J Y, LI Y X, WANG W S. Microstructure and properties of electronic packaging box with high silicon aluminum-base alloy by semi-solid thixoforming [J]. *Transactions of Nonferrous Metals Society of China*, 2013, 23(1): 80–85.

[4] TOKUNAGA T, KANEKO K, SATO K, HORITA Z. Microstructure and mechanical properties of aluminum–fullerene composite fabricated by high pressure torsion [J]. *Scripta Materialia*, 2008, 58(9): 735–738.

[5] KHALID F A, BEFFORT O, KLOTZ U E, KELLER B A, GASSER P, VAUCHER S. Study of microstructure and interfaces in an aluminium–C60 composite material [J]. *Acta Materialia*, 2003, 51(15): 4575–4582.

[6] BAKSHI S R, SINGH V, SEAL S, AGARWAL A. Aluminum composite reinforced with multiwalled carbon nanotubes from plasma spraying of spray dried powders [J]. *Surface and Coatings Technology*, 2009, 203(10–11): 1544–1554.

[7] BAKSHI S R, SINGH V, BALANI K, MCCARTNEY D G, SEAL S, AGARWAL A. Carbon nanotube reinforced aluminum composite coating via cold spraying [J]. *Surface and Coatings Technology*, 2008, 202(21): 5162–5169.

[8] KESHRI A K, BALANI K, BAKSHI S R, SINGH V, LAHA T, SEAL S, AGARWAL A. Structural transformations in carbon nanotubes during thermal spray processing [J]. *Surface and Coatings Technology*, 2009, 203(16): 2193–2201.

[9] UOZUMI H, KOBAYASHI K, NAKANISHI K, MATSUNAGA T, SHINOZAKI K, SAKAMOTO H, TSUKADA T, MASUDA C, YOSHIDA M. Fabrication process of carbon nanotube/light metal matrix composites by squeeze casting [J]. *Materials Science and Engineering A*, 2008, 495(1–2): 282–287.

[10] GOH C S, WEI J, LEE L C, GUPTA M. Ductility improvement and fatigue studies in Mg-CNT nanocomposites [J]. *Composites Science and Technology*, 2008, 68(6): 1432–1439.

[11] PARAMSOTHY M, HASSAN S F, SRIKANTH N, GUPTA M. Adding carbon nanotubes and integrating with AA5052 aluminium alloy core to simultaneously enhance stiffness, strength and failure strain of AZ31 magnesium alloy [J]. *Composites Part A: Applied Science and Manufacturing*, 2009, 40(9): 1490–1500.

[12] LIM D K, SHIBAYANAGI T, GERLICH A P. Synthesis of multi-walled CNT reinforced aluminium alloy composite via friction stir processing [J]. *Materials Science and Engineering A*, 2009, 507(1–2): 194–199.

[13] ESAWI A M K, EL BORADY M A. Carbon nanotube-reinforced aluminium strips [J]. *Composites Science and Technology*, 2008, 68(2): 486–492.

[14] CHOI H, KWON G, LEE G, BAE D. Reinforcement with carbon nanotubes in aluminum matrix composites [J]. *Scripta Materialia*, 2008, 59(3): 360–363.

[15] ESAWI A M K, MORSI K, SAYED A, GAWAD A A, BORAH P. Fabrication and properties of dispersed carbon nanotube–aluminum composites [J]. *Materials Science and Engineering A*, 2009, 508(1–2): 167–173.

[16] CHOI H J, SHIN J H, BAE D H. The effect of milling conditions on microstructures and mechanical properties of Al/MWCNT composites [J]. *Composites Part A: Applied Science and Manufacturing*, 2012, 43(7): 1061–1072.

[17] PÉREZ-BUSTAMANTE R, GÓMEZ-ESPARZA C D, ESTRADA-GUEL I, MIKI-YOSHIDA M, LICEA-JIMÉNEZ L, PÉREZ-GARCÍA S A, MARTINEZ-SÁNCHEZ R. Microstructural

- and mechanical characterization of Al-MWCNT composites produced by mechanical milling [J]. *Materials Science and Engineering A*, 2009, 502(1-2): 159-163.
- [18] BARTOLUCCI S F, PARAS J, RAFIEE M A, RAFIEE J, LEE S, KAPOOR D, KORATKAR N. Graphene-aluminum nanocomposites [J]. *Materials Science and Engineering A*, 2011, 528(27): 7933-7937.
- [19] WANG J, LI Z, FAN G, PAN H, CHEN Z, ZHANG D. Reinforcement with graphene nanosheets in aluminum matrix composites [J]. *Scripta Materialia*, 2012, 66(8): 594-597.
- [20] KOMATSU K, MURATA M, MURATA Y. Encapsulation of molecular hydrogen in fullerene C60 by organic synthesis [J]. *Science*, 2005, 307(5707): 238-240.
- [21] BRIGGS J B, MILLER G P. [60]Fullerene-acene chemistry: A review [J]. *Comptes Rendus Chimie*, 2006, 9(7-8): 916-927.
- [22] AHN J H, SHIN H S, KIM Y J, CHUNG H. Structural modification of carbon nanotubes by various ball milling [J]. *Journal of Alloys and Compounds*, 2007, 434-435: 428-432.
- [23] QIAO L, SUN X, YANG Z, WANG X, WANG Q, HE D. Network structures of fullerene-like carbon core/nano-crystalline silicon shell nanofibers as anode material for lithium-ion batteries [J]. *Carbon*, 2013, 54: 29-35.
- [24] LI G, HAN Z, PIAO G, ZHAO J, LI S, LIU G. To distinguish fullerene C60 nanotubes and C60 nanowhiskers using Raman spectroscopy [J]. *Materials Science and Engineering: B*, 2009, 163(3): 161-164.
- [25] TARANTILI P A, ANDREOPOULOS A G, GALIOTIS C. Real-time micro-Raman measurements on stressed polyethylene fibers: 1. Strain rate effects and molecular stress redistribution [J]. *Macromolecules*, 1998, 31(20): 6964-6976.
- [26] COURTNEY T H. *Mechanical behavior of materials* [M]. Singapore: McGraw-Hill Co., 2000: 26.
- [27] CHOI H. Reinforcing effects of carbon nanotubes in aluminum matrix composites [D]. Korea: Yonsei University, 2010.
- [28] CHOI H J, SHIN J H, BAE D H. Grain size effect on the strengthening behavior of aluminum-based composites containing multi-walled carbon nanotubes [J]. *Composites Science and Technology*, 2011, 71(15): 1699-1705.

## 富勒烯增强铝基纳米复合材料的力学性能

Kwangmin CHOI<sup>1</sup>, Jiyeon SEO<sup>2</sup>, Donghyun BAE<sup>2</sup>, Hyunjoo CHOI<sup>1</sup>

1. School of Advanced Materials Engineering, Kookmin University, Seoul 136-702, Korea;

2. School of Advanced Materials Engineering, Yonsei University, Seoul 120-749, Korea

**摘要:** 研究了富勒烯在铝基复合材料中的增强作用。该复合材料采用二次球磨结合热轧制技术制备。最初，富勒烯是由富勒烯分子通过范德华力结合在一起形成大的颗粒(~200 μm)，首先，通过行星球磨将大的颗粒破碎成更小的颗粒(~1 μm)；然后，采用高能球磨将富勒烯粉末分散在铝粉中；最后，将富勒烯/铝复合粉体在 480 °C 热轧成板材。由于富勒烯的晶粒细化和弥散强化作用，2%(体积分数)的富勒烯/铝复合材料板材表现出高的维氏硬度(HV ~222)和高的屈服强度(~740 MPa)。

**关键词:** 铝；富勒烯；球磨；粉末冶金；复合材料

(Edited by Bing YANG)